

# Characterization of Electrochemical Sensors Based on Carbon Nanotubes and MIPS for Determination of Ferulic Acid <sup>†</sup>

Miguel S. P. de Sousa <sup>1</sup>, Acelino C. de Sá <sup>2</sup> and Leonardo L. Paim <sup>1,\*</sup>

<sup>1</sup> Engineering of Energy, Campus of Rosana, São Paulo State University (UNESP), Barrageiros Avenue 1881, Rosana 19274-000, Brazil; miguel.sales@unesp.br

<sup>2</sup> Institute of Physics, São Carlos, USP—University of São Paulo, São Carlos 13560-970, Brazil; acelino2@hotmail.com

\* Correspondence: leonardo.paim@unesp.br

<sup>†</sup> Presented at the 2nd Coatings and Interfaces Web Conference, 15–31 May 2020; Available online: <https://ciwc2020.sciforum.net/>.

Published: 14 May 2020

**Abstract:** In order to mitigate the impacts caused by the rampant consumption of fossil fuels, many countries are investing in the development and optimization of alternatives that minimize dependence on fossil energy. The second generation of ethanol (2G), characterized by its relevant production potential, is considered a good alternative, which can be produced from sugarcane bagasse. Therefore, it is extremely important to evaluate the efficiency of 2G ethanol production processes, mainly in the compositional analysis of hydrolysates from the pre-treatment of lignocellulosic biomass, to promote greater production. Thus, the development of electrochemical sensors composed of graphite/paraffin composite electrodes coated with multi-walled carbon nanotubes (MWCNTs) modified with molecularly imprinted polymers (MIPs) are an excellent option for carrying out rapid analyzes. Due to the highly sensitive electrical properties of the MWCNTs and the molecular impression of the polymers that allow a high affinity with the model molecule, the sensor has high selectivity, good sensitivity and reproducibility for the determination of ferulic acid. For this reason, the present work, using the Scanning Electron Microscopy (SEM) and Cyclic Voltammetry (CV) technique, presents remarkable morphological characteristics of the sensor surface and its electrochemical behavior in relation to the electropolymerization process and speed increase of the scan.

**Keywords:** ferulic acid; electrochemical sensor; ethanol 2G

---

## 1. Introduction

The unbridled consumption of fossil fuels causes serious impacts on the environment. Thus, alternatives are developed and optimized to mitigate the effect of fossil energy use in the world [1]. Biofuels are considered relevant alternatives to supply or at least decrease dependence on fossil sources, seen by the possibility of increasing energy conversion efficiency [1].

First-generation (1G) ethanol is a good option, but the use of edible sources for its production ends up influencing its viability [2]. Thus, the production of second-generation (2G) ethanol becomes an attractive option, seen through the use of lignocellulosic biomass, which does not compete with food sources [2]. However, the efficiency of the technology used in the processes to obtain 2G ethanol is not efficient when compared to 1G ethanol, which is mainly due to the composition of biomass, defined by cellulose and hemicellulose strongly linked by lignin [3].

Therefore, it is extremely important to evaluate the efficiency of 2G ethanol production processes, mainly in the compositional analysis of hydrolysates from the pre-treatment of lignocellulosic biomass, to increase production. Thus, the development of electrochemical sensors modified with functionalized multi-walled carbon nanotubes (FMWCNTs) and with molecularly imprinted polymers (MIPs) for the determination of ferulic acid is an excellent option.

The FMWCNTs coating endows the electrode with a high sensitivity due to the electrical and thermal properties of the carbon nanotubes [4]. In addition, the formation of a polymer film on the electrode surface containing molecular recognition sites confers selectivity to the sensor [5].

## 2. Materials and Methods

Acetic acid (purity: 97.3%), ferulic acid (purity:  $\geq 99.0\%$ ), o-Phenylenediamine (flaked, 99.5%), nitric acid (purity:  $\geq 98.0\%$ ), dimethylformamide (purity:  $\geq 98.9\%$ ) and graphite ( $< 20\ \mu\text{m}$ , synthetic), were purchased from Sigma-Aldrich. Sodium acetate (purity:  $\geq 99.0\%$ ), potassium chloride (purity:  $\geq 99.0\%$ ), potassium ferrocyanide (purity:  $\geq 99.5\%$ ) and histological paraffin ( $56\text{--}58\ ^\circ\text{C}$ ), were purchased from Synth. The oxidation probe solution was  $10.0 \times 10^{-3}\ \text{mol L}^{-1}\ \text{K}_3[\text{Fe}(\text{CN})_6]$  in  $1.0\ \text{mol L}^{-1}\ \text{KCl}$ . Electrochemical measurements were performed with the Potentiostat/Galvanostat PGSTAT204 (Autolab, Metrohm, Ionenstrasse, Switzerland). A conventional three-electrode system was used, with Ag/AgCl as the reference electrode, platinum electrode as counter-electrode and modified working electrode. In order to characterize the surface morphology of the work electrodes, the JEOL JSM-7500F equipment was used. All experiments were carried out at room temperature.

The substrates were prepared from a graphite/paraffin mixture in the proportion of 7:3 (*v/v*), similar to that described in the literature [6,7]. The modification of the electrode surface is carried out by electrodeposition of FMWCNTs in the range of  $-0.5$  to  $1.0\ \text{V}$  for 15 consecutive cycles at a scanning speed of  $50\ \text{mVs}^{-1}$  [8–10]. This can also be achieved by electropolymerization of MIPs in a range of  $-0.4$  to  $1.0\ \text{V}$  for 20 cycles, with a speed of  $50\ \text{mV}^{-1}$  in a standard acetate solution with pH 5.0 containing  $5.0 \times 10^{-3}\ \text{mol L}^{-1}$  o-PD and  $9.0 \times 10^{-4}\ \text{mol L}^{-1}$  of ferulic acid, similarly to the literature [8,11]. For the extraction step the dimethylformamide/acetic acid solution (5:2, *v/v*) is used, where the modified electrodes are immersed for 60 s. Afterwards, the adsorption process is performed, where the sensor is immersed in a standard acetate solution with pH 5.0 containing  $9.0 \times 10^{-4}\ \text{mol L}^{-1}$  of ferulic acid for 7 min, in order to fill the cavities left after the extraction step. Figure 1 presents the processes that constituted the manufacture of the electrochemical sensor.

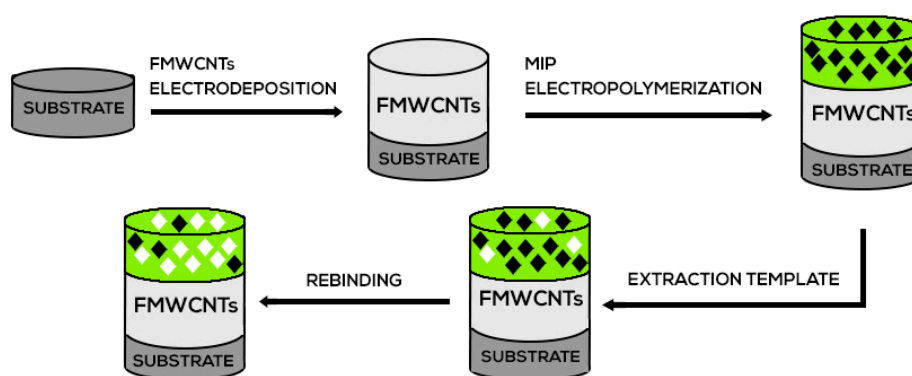


**Figure 1.** Representation of the manufacture of the electrochemical sensor for the determination of ferulic acid.

## 3. Results and Discussion

### 3.1. Electrochemical Characterization

The MIP technology has been widely used due to its excellent properties such as low cost, high selectivity and sensitivity [12]. The molecularly imprinted polymers have characteristics of the target molecule, which allows the detection of this molecule even in a solution containing interferents

[13,14]. The formation of the MIP comes from the polymerization in solution of monomers and reticulators, so that after the polymerization the extraction process allows the establishment of sites, with size and features which are characteristic of the analyte [13,14].

In Figure 2, the process of forming the MIP on the surface of the working electrode is shown; 20 cycles are required for the formation of the non-conducting polymeric film. In the first cycle, a high current peak is identified, and during the other cycles a decrease in current is recorded, which indicates the formation of the film.

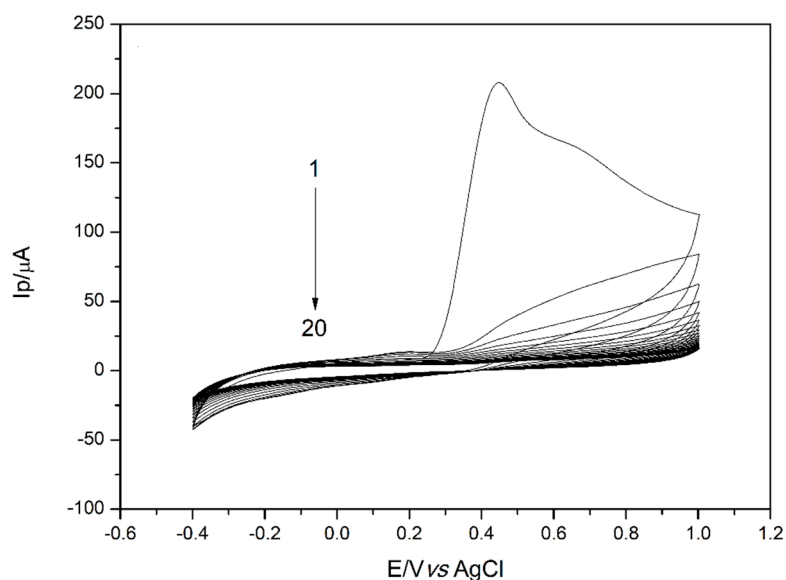


**Figure 2.** Cyclic voltammograms from the electropolymerization process on the surface of the working electrode.

The formation of a diffuse layer through the interaction between the electrode and the electrolytic solution containing the ferulic acid analyte can be followed by changes in the Helmholtz double layer, where the electroactive molecules are attracted to the electrode by interactions of long distances [15,16]. Thus, in Figure 3 a relationship is shown between the increase of the peak current and the increase of the scanning speed, this is due to the size of the diffuse layer, where a speed increase causes a decrease of the layer thickness, leading to interactions of smaller hydration radius.

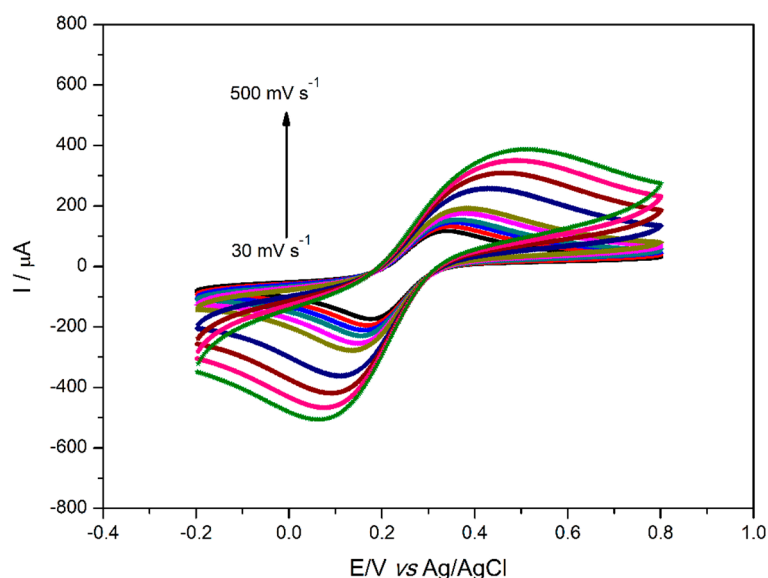


**Figure 3.** Cyclic voltammograms with scanning speeds of 30, 40, 50, 60, 80, 100, 200, 300, 400, 500  $\text{mV s}^{-1}$ .

The influence of speed on the peak of anode and cathode currents is shown in Figure 4.

In Figure 4A the current peaks are not proportional to the scanning speed, the anodic peak is expressed by  $I (\mu\text{A}) = 0.3065v + 149.724$  ( $R = 0.9461$ ), and the cathode peak by  $I (\mu\text{A}) = -0.4184v - 167.808$  ( $R = 0.9503$ ), indicating a diffusion controlled system [17]. On the contrary, in Figure 4B, the currents are proportional to the square root of the scanning speed, where the anode peak current is expressed by:  $I (\mu\text{A}) = 8.7690v + 98.980$  ( $R = 0.985$ ) and the cathode peak current by  $I (\mu\text{A}) = -98.812v - 11.947$  ( $R = 0.987$ ), being characterized by diffusion.

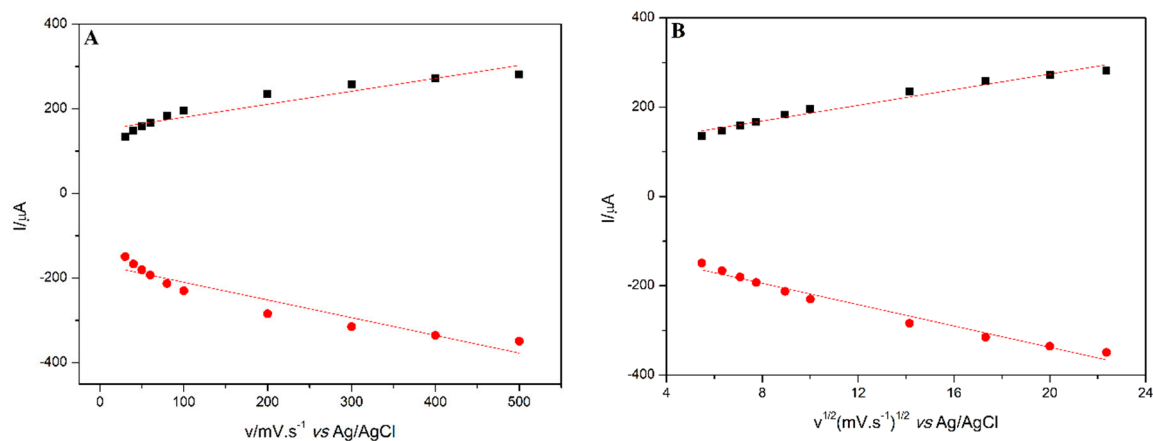


**Figure 4.** (A) Influence of the scanning speed under the peak currents of MIP ferulic acid; (B) Influence of the square root of the scanning speed under the peak currents of MIP ferulic acid.

### 3.2. Morphological Characterization

The surface morphology of the electrochemical sensor modified with FMWCNTs and MIP-FA was investigated by Scanning Electron Microscopy (SEM). In Figure 5A,B, the carbon nanotubes and the polymeric film can be identified. Interestingly, the cylindrical and entangled features characteristics of FMWCNTs, which have excellent electrical conductivity, high chemical stability, high surface area, good mechanical and thermal properties [18,19].

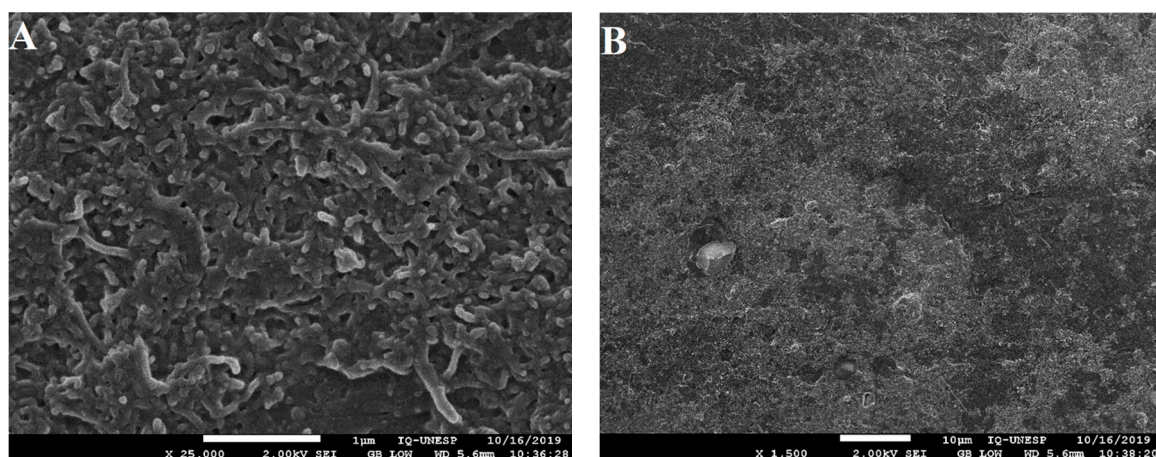


**Figure 5.** (A,B) SEM images of the surface morphology of the electrochemical sensor modified with FMWCNTs and MIP-FA.

## 4. Conclusions

The characterization of the electrochemical sensor based on FMWCNTs and MIPs for determination of ferulic acid, performed by SEM and CV techniques, shows the electrochemical behavior of the sensor during the formation of the polymeric film with the ferulic acid molecule, something little seen in the literature. In addition, the study of speed is applied, resulting in a system

controlled by diffusion. Additionally, remarkable morphological characteristics of the sensor surface confirm the modifications made.

**Funding:** This research was funded by the São Paulo Research Foundation (FAPESP) (Proc. No. 2017/09123-9).

**Conflicts of Interest:** The authors declare no conflict of interest.

## References

1. Manochio, C.; Andrade, B.R.; Rodriguez, R.P.; Moraes, B.S. Ethanol from biomass: A comparative overview. *Renew. Sustain. Energy Rev.* **2017**, *80*, 743–755, doi:10.1016/j.rser.2017.05.063.
2. Zabed, H.; Sahu, J.N.; Suely, A.; Boyce, A.N.; Faruq, G. Bioethanol production from renewable sources: Current perspectives and technological progress. *Renew. Sustain. Energy Rev.* **2017**, *71*, 475–501, doi:10.1016/j.rser.2016.12.076.
3. Zabed, H.; Sahu, J.N.; Boyce, A.N.; Faruq, G. Fuel ethanol production from lignocellulosic biomass: An overview on feedstocks and technological approaches. *Renew. Sustain. Energy Rev.* **2016**, *66*, 751–774, doi:10.1016/j.rser.2016.08.038.
4. Ho, K.C.; Teow, Y.H.; Mohammad, A.W.; Ang, W.L.; Lee, P.H. Development of graphene oxide (GO)/multi-walled carbon nanotubes (MWCNTs) nanocomposite conductive membranes for electrically enhanced fouling mitigation. *J. Membr. Sci.* **2018**, *552*, 189–201, doi:10.1016/j.memsci.2018.02.001.
5. Ahmad, O.S.; Bedwell, T.S.; Esen, C.; Garcia-Cruz, A.; Piletsky, S.A. Molecularly Imprinted Polymers in Electrochemical and Optical Sensors. *Trends Biotechnol.* **2019**, *37*, 294–309, doi:10.1016/j.tibtech.2018.08.009.
6. Alizadeh, T.; Ganjali, M.R.; Norouzi, P.; Zare, M.; Zeraatkar, A. A novel high selective and sensitive para-nitrophenol voltammetric sensor, based on a molecularly imprinted polymer–carbon paste electrode. *Talanta* **2009**, *79*, 1197–1203, doi:10.1016/j.talanta.2009.02.051.
7. Du, D.; Chen, S.; Cai, J.; Tao, Y.; Tu, H.; Zhang, A. Recognition of dimethoate carried by bi-layer electrodeposition of silver nanoparticles and imprinted poly-o-phenylenediamine. *Electrochim. Acta* **2008**, *53*, 6589–6595, doi:10.1016/j.electacta.2008.04.027.
8. Sousa, M.S.P.; de Sá, A.C.; de Oliveira, J.P.J.; de Silva, M.J.; da Santos, R.J.; Paim, L.L. Impedimetric Sensor for Pentoses Based on Electrodeposited Carbon Nanotubes and Molecularly Imprinted poly-o-phenylenediamine. *ECS J. Solid State Sci. Technol.* **2020**, *9*, 041006, doi:10.1149/2162-8777/AB85BD.
9. Chen, L.; Tang, Y.; Wang, K.; Liu, C.; Luo, S. Direct electrodeposition of reduced graphene oxide on glassy carbon electrode and its electrochemical application. *Electrochem. Commun.* **2011**, *13*, 133–137, doi:10.1016/j.ELECOM.2010.11.033.
10. Guzmán, M.G.; Dille, J.; Godet, S. Synthesis of silver nanoparticles by chemical reduction method and their antibacterial activity. *Int. J. Mater. Metall. Eng.* **2008**, *2*, 91–98, doi:10.5281/zenodo.1062628.
11. Wang, Q.; Paim, L.L.; Zhang, X.; Wang, S.; Stradiotto, N.R. An Electrochemical Sensor for Reducing Sugars Based on a Glassy Carbon Electrode Modified with Electropolymerized Molecularly Imprinted Poly-o-phenylenediamine Film. *Electroanalysis* **2014**, *26*, 1612–1622, doi:10.1002/elan.201400114.
12. Gui, R.; Jin, H.; Guo, H.; Wang, Z. Recent advances and future prospects in molecularly imprinted polymers-based electrochemical biosensors. *Biosens. Bioelectron.* **2018**, *100*, 56–70, doi:10.1016/j.bios.2017.08.058.
13. Turiel, E.; Martín-Esteban, A. Molecularly imprinted polymers-based microextraction techniques. *TrAC Trends Anal. Chem.* **2019**, *118*, 574–586, doi:10.1016/j.trac.2019.06.016.
14. Ashley, J.; Shahbazi, M.A.; Kant, K.; Chidambara, V.A.; Wolff, A.; Bang, D.D.; Sun, Y. Molecularly imprinted polymers for sample preparation and biosensing in food analysis: Progress and perspectives. *Biosens. Bioelectron.* **2017**, *91*, 606–615, doi:10.1016/j.bios.2017.01.018.
15. Yates, D.E.; Levine, S.; Healy, T.W. Site-binding model of the electrical double layer at the oxide/water interface. *J. Chem. Soc. Faraday Trans. 1 Phys. Chem. Condens. Phases* **1974**, *70*, 1807–1818, doi:10.1039/F19747001807.
16. Grahame, D.C.; Soderberg, B.A. Ionic components of charge in the electrical double layer. *J. Chem. Phys.* **1954**, *22*, 449–460, doi:10.1063/1.1740089.
17. Bard, A.J.; Faulkner, L.R. *Electrochemical Methods: Fundamentals and Applications*, 2nd ed.; Wiley: New York, NY, USA, 2001.

18. El-Wakil, M.M.; Darweesh, M.; Shaykoon, M.S.A.; Ali, R. Enzyme-free and label-free strategy for electrochemical oxaliplatin aptasensing by using rGO/MWCNTs loaded with AuPd nanoparticles as signal probes and electro-catalytic enhancers. *Talanta* **2020**, 121084, doi:10.1016/j.talanta.2020.121084.
19. Xue, S.M.; Xu, Z.L.; Tang, Y.J.; Ji, C.H. Polypiperazine-amide Nanofiltration Membrane Modified by Different Functionalized Multiwalled Carbon Nanotubes (MWCNTs). *ACS Appl. Mater. Interfaces* **2016**, 8, 19135–19144, doi:10.1021/acsami.6b05545.



© 2020 by the authors. Licensee MDPI, Basel, Switzerland. This article is an open access article distributed under the terms and conditions of the Creative Commons Attribution (CC BY) license (<http://creativecommons.org/licenses/by/4.0/>).